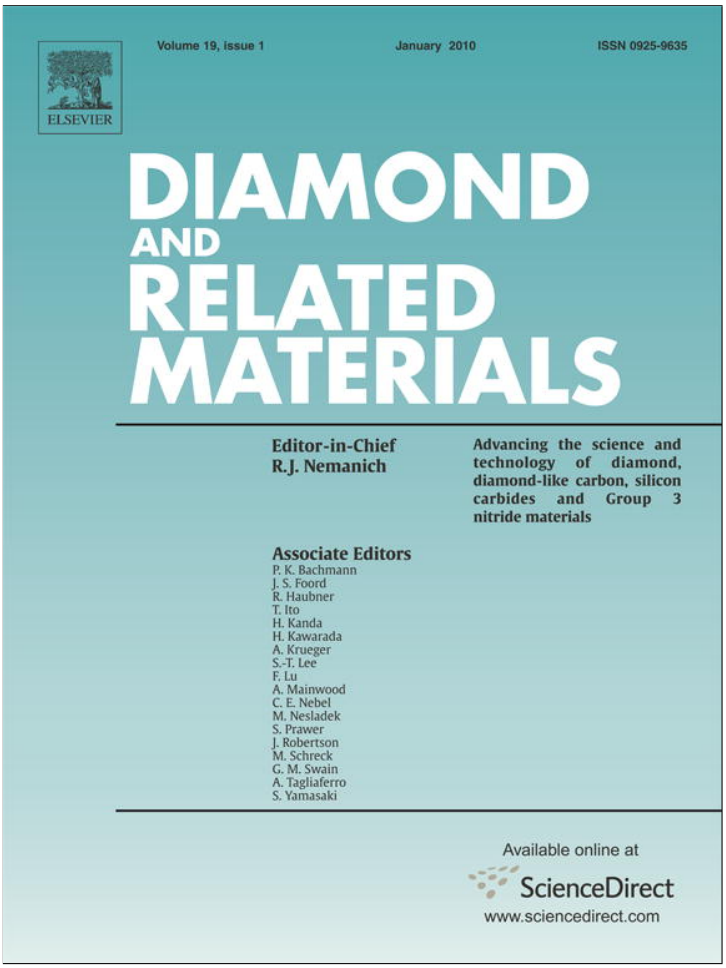

Diamond & Related Materials 19 (2010) 7–14

Contents lists available at ScienceDirect

Diamond & Related Materials

journal homepage: www.elsevier.com/locate/diamond

Pulsed laser deposition of hard and superhard carbon thin films from C_{60} targets

J.V. Rau [a,*], R. Teghil [b], A. De Bonis [b], A. Generosi [a], B. Paci [a], R. Generosi [a], M. Fosca [a], D. Ferro [c], V. Rossi Albertini [a], N.S. Chilingarov [d]

[a] Istituto di Struttura della Materia, CNR, Via del Fosso del Cavaliere, 100-00133, Rome, Italy
[b] Università della Basilicata, Dipartimento di Chimica, via N. Sauro 85 – 85100, Potenza, Italy
[c] Istituto per lo Studio dei Materiali Nanostrutturati, CNR, P.le Aldo Moro 5 – 00185, Rome, Italy
[d] "Lomonosov" Moscow State University, Chemistry Department, Leninskije Gory, Moscow, Russia

ARTICLE INFO

Article history:
Received 24 June 2009
Received in revised form 28 September 2009
Accepted 7 October 2009
Available online 29 October 2009

Keywords:
Fullerenes
Diamond-like carbon
Films
Pulsed laser deposition
Characterization
Hardness
Superhard materials

ABSTRACT

In the present study, carbon films were deposited by a pulsed laser deposition method. A C_{60} fullerene target has been irradiated by a frequency doubled Nd:YAG laser with a pulse duration of 7 ns. The carbon films grown on Si(111) substrates at different substrate deposition temperatures (30, 300 and 500 °C) were characterized by Raman, X-ray Photoelectron and X-ray Auger Electron Spectroscopies, Energy Dispersive X-Ray Diffraction, Scanning Electron and Atomic Force Microscopies, and Vickers microhardness technique. The composition, structure, morphology and mechanical properties of films were found to be strongly dependent on the substrate temperature. At 30 °C and 300 °C deposition temperature, superhard and hard diamond-like films have been obtained, respectively. In the case of 500 °C deposition, a hard film, composed of crystalline C_{60} and diamond-like carbon, has been prepared.

1. Introduction

Pulsed Laser Deposition (PLD) is proved to be a versatile and powerful technique for preparation of a great variety of films. This technique is suitable not only to deposit films, maintaining the stoichiometry and properties of bulk target, but also to produce the coatings with the desired properties, quite different from those of the starting material. Carbon, exhibiting several allotropic states, is a very good example to demonstrate the latter statement. For instance, one of the many forms of carbon, diamond-like carbon (DLC), otherwise called tetrahedral amorphous carbon, could be obtained by laser vaporization of graphite [1].

Amorphous DLC materials, at the atomic level, represent a material with strong chemical bonding composed of the mixture of sp^3 and sp^2 arrangements of atoms incorporated into an amorphous carbon matrix. Theoretical models of this structure were proposed in [2,3]. Controlling the sp^3/sp^2 ratio, DLC properties could be tailored, and high quality DLC could rival properties of the crystalline diamond. PLD has been successfully applied to deposit DLC films typically from graphite, polycarbonate and C_{60} targets [4–7]. Coatings, consisting of carbon materials with structures and properties varying from graphite-like to diamond-like, depending on laser output parameters, background environment and substrate temperature, as described in literature, were obtained [4,8]. By the proper selection of PLD parameters, DLC coatings of different hardness (from moderate to superhard) can be produced. According to the literature [6], low substrate temperature is required to grow amorphous DLC coatings, while at temperatures above 150–200 °C, graphite-like coatings can be prepared.

DLC films have been extensively studied due to their excellent mechanical properties and their high potential in various industrial applications. In 2006, the market for outsourced DLC coatings was estimated to be about 30,000,000 € in the European Union. Diamond-like carbon coatings exhibit a number of exceptional properties, such as high density and electrical resistivity, chemical inertness, IR transparency, high elastic modulus and elevated hardness. They have a broad range of applications varying from wear-resistant and low friction coefficient protective coatings. Furthermore, DLC coatings were found to be biocompatible and suitable for potential use in biomedical applications [9,10].

Another type of carbon materials, such as fullerenes, synthesized in macroscopic quantities only in 1990 [11], could also be obtained as films by the Pulsed Laser Deposition method. The unique structure of C_{60} and its derivatives have great technological potential in a wide area, such as semiconductors, superconductors, electronic and optical devices [12–15], C_{60}-based solar cells [16], and C_{60}-based devices for space application [17]. Furthermore, microstructured fullerene layers

* Corresponding author. Istituto di Struttura della Materia, Consiglio Nazionale delle Ricerche, (CNR), Via del Fosso del Cavaliere, 100 – 00133 Rome, Italy. Tel.: +39 06 4993 4124; fax: +39 06 4993 4153.
E-mail address: giulietta.rau@ism.cnr.it (J.V. Rau).

0925-9635/$ – see front matter © 2009 Elsevier B.V. All rights reserved.
doi:10.1016/j.diamond.2009.10.010

could be used as a bioactive coating for bone implants providing good cell adhesion and growth and good integration with the surrounding tissue [18].

The present work provides a comparative study of carbon films produced by PLD from a C_{60} fullerene target over a wide range of substrate temperatures (30–500 °C). The films obtained under the same laser output conditions are of a rather different nature: those deposited at 30 and 300 °C are composed of amorphous DLC, while at 500 °C the films contain both crystalline C_{60} and DLC contribution. The properties of the deposited films were investigated by Raman, X-ray Photoelectron and X-ray Auger Electron Spectroscopies (XPS and XAES), Energy Dispersive X-Ray Diffraction (EDXRD), Scanning Electron and Atomic Force Microscopies (SEM and AFM), and Vickers microhardness technique.

2. Material and methods

2.1. Pulsed Laser Deposition procedure

The C_{60} target was prepared by cold pressing a C_{60} powder (99.98%, Term-USA) into a pellet. The films were deposited on Si(111) substrates at different substrate temperatures, namely: 30, 300, and 500 °C.

The ablations were performed in a stainless steel vacuum chamber, evacuated down to a pressure of 1.5×10^{-4} Pa, equipped with a rotating target holder and a heatable substrate support. The laser beam was oriented with an inclination angle of 45° with respect to the target, while substrate and target were assembled in a frontal geometry at 2 cm of reciprocal distance. Depositions in the nanosecond regime were carried out by focusing a frequency doubled Nd:YAG laser ($\lambda = 532$ nm emission wavelength, pulse duration = 7 ns, repetition rate = 10 Hz) on the pressed C_{60} rotating target, the rotation being necessary to ensure homogeneous ablation of the material. The highest spot energy fluence was 18.0 J/cm^2, and the total deposition time was 2 h.

2.2. Film structure and properties characterization

2.2.1. Raman Spectroscopy

Raman spectra were recorded in a backscattered configuration using a Jobin Yvon LABRAM HR 800 microRaman-spectrometer, equipped with two gratings (600 g/mm and 1800 g/mm) and with an Olympus microscope supplied with 10×, 50× and 100× objectives. The spectrometer was connected to a CCD detector. Excitations were performed with 632.8 nm radiation from a He–Ne laser source. The laser power was maintained at 20 mW. The spectra were acquired using the 600 g/mm grating and the 100× objective. In these conditions, the estimated resolution was around 4 cm^{-1}.

2.2.2. X-ray Photoelectron and X-ray Auger Electron Spectroscopies

X-ray Photoelectron and X-ray Auger Electron emission spectra were acquired by a LH-Leybold X1 spectrometer using a non-monochromatized MgKα radiation operating at a constant power of 260 W. Wide and detailed spectra were collected in FAT mode with a pass energy of 50 eV and a channel widths of 1.0 and 0.1 eV, respectively. The acquired XPS spectra were analyzed using a curve-fitting program, Googly, described in [19], which allows the simultaneous fitting of photo-peaks in the form of a Voigt function and their associated background in a wide energy range. Derivative XAES spectra were obtained using a 23-point Savitzky–Golay convolution array. A second-order polynomial was used in the Savitzky–Golay analysis.

2.2.3. Energy Dispersive X-Ray Diffraction

The EDXRD experimental apparatus consisted of a non-commercial diffractometer [20] making use of a non-monochromatized primary beam. After the interaction with the sample, the X-ray beam was analyzed by a solid-state detector (SSD), capable of performing the energy scan of the diffracted photons. The set-up is characterized by a very simple geometry, since neither monochromator nor goniometer are required in the Energy Dispersive mode, no movement being needed during the measurements. The Bremmsstrahlung used as a probe is produced by a 3 kW power, tungsten anode X-ray tube. An EG&G high purity germanium solid-state detector, whose energy resolution is about 1.5–2% in the 20–50 keV energy range, accomplishes the energy scan.

The advantages of the Energy Dispersive method, with respect to the conventional Angular Dispersive one, was discussed in detail in [21]. Furthermore, a Rocking Curve (RC) analysis was carried out by recording for each film the intensity of the diffracted radiation as a function of an asymmetry parameter $\alpha = (\vartheta_i - \vartheta_f)/2$, where ϑ_i and ϑ_f are the initial (incidence) and final (deflection) angles, and $\vartheta_i + \vartheta_f = 2\vartheta$ is kept constant [22].

2.2.4. Scanning Electron Microscopy

Scanning Electron Microscopy (a LEO 1450 Variable Pressure apparatus), working in secondary and backscattered electron modes, was used for morphological studies of the deposited films. SEM apparatus was coupled with a system for microanalysis EDXRS (Energy Dispersive X-Ray Spectroscopy) INCA 300 that allows executing qualitative/quantitative analysis of the elements, starting from atomic number 5 (Boron) with a sensitivity limit of about 0.2%. The resolution of the apparatus in vacuum conditions was about 4 nm. Both plane and cross section view images of the film samples were obtained, the latter being necessary for thickness measurements. Since the images of the film cross sections were obtained by tilting the samples at 45°, the measured thickness values were multiplied by $\sqrt{2}/2$. The film thickness measurements were carried out in the backscattered electron mode by means of the 4 Quadrants detector. The atomic number contrast, presented in the SEM images as grey colour hues, allowed to precisely distinguish the film boundary and the interface with the Si(111) substrate. To confirm the results of the atomic number contrast, the EDXRS analysis of the chemical nature of the observed phases has been carried out.

2.2.5. Atomic Force Microscopy

The AFM measurements were performed in a non-contact mode using a non-commercial air-operating atomic force microscope [23]. Several portions of the film sample surfaces were topographically/phase-shift reconstructed in order to evaluate the morphological/chemical homogeneity of the depositions. The topographic images (3 μm × 3 μm and 2 μm × 2 μm) were collected from the representative portions of the films in order to quantitatively evaluate the surface texture, roughness and the aggregate dimensions. To estimate the film thickness, a scratch was made in the film layer and its profile was measured in a contact mode.

2.2.6. Vickers microhardness measurements

Microhardness measurements were performed by means of a Leica VMHT apparatus (Leica GmbH, Germany) equipped with a standard Vickers pyramidal indenter (square-based diamond pyramid of 136° face angle). The loading and unloading speed was 5×10^{-6} m/s, and the time under the peak load was 15 s. The hardness of the Si(111) substrate and of the deposited films was measured according to the procedure described in detail in our previous works [24,25].

For film samples, the measured hardness was that of the film/substrate composite system. To separate the composite hardness of the film/substrate system (H_c) into its components, film (H_f) and substrate (H_s), a Jönsson and Hogmark model based on area "law-of-mixtures" approach was applied [26], taking into account the indentation size effect [27]. In this case, composite hardness H_c is expressed as:

$$H_c = H_{s0} + [B_s + 2ct(H_{f0} - H_{s0})] / D, \quad (1)$$

where $c \cong 0.5$ for a brittle hard film on a more ductile substrate [26]; H_{s0} and H_{f0} are the intrinsic hardness of substrate and film, respectively; t is film thickness; D is the indentation diagonal, and B_s is a coefficient, which can be deduced from substrate hardness measurements.

To evaluate H_{s0} and B_s values, the hardness of the Si(111) substrate was measured first. The relation between the measured substrate hardness, H_s, and the reciprocal length of the indentation imprints is expressed by the following equation [28]:

$$H_s = H_{s0} + B_s / D. \quad (2)$$

The values obtained for the Si(111) substrate, H_{s0} and the B_s coefficient, are equal to 8.3 ± 0.5 GPa and $(26.8 \pm 3.5) \times 10^{-6}$ GPa m, respectively.

To calculate the intrinsic hardness of films, special attention was paid to choose correctly the indentation depths, $d = D/7$ (for Vickers pyramidal indenter), i.e. in the range, where the applied model is valid. The $d/t = D/7t$ range for the deposited films was (0.9–3.6), perfectly in the range of substrate-dominated mixed region, where the film is fractured conforming to the plastically deforming substrate [29]. In this d/t range, the results obtained using the Jönsson and Hogmark model have been demonstrated to coincide quite well with estimations resulting from more complicated models [29,30].

For hardness measurements on the film/Si(111) substrate system, indentations were made applying 4 loads ranging from 0.147 up to 0.981 N. For each sample, approximately 10 indentations were made at each load. Application of higher loads led to the film cracking.

3. Results and discussion

Raman scattering applied in this work is a powerful tool to investigate the various carbon materials. From the characteristic Raman spectra, the structure and bonding configurations of carbon can be deduced. In Fig. 1(A), the Raman spectra of the films deposited at 30, 300 and 500 °C are presented. As one can see, the film deposited at 30 °C shows a broad band in the range of 1200–1700 cm^{-1} centered at about 1490 cm^{-1}, and a sharp peak at 520 cm^{-1}, this latter coming from the Si substrate. The broad band is likely a convolution of two peaks: G-band (1580 cm^{-1}) and D-band (1350 cm^{-1}), typical for amorphous diamond-like carbon films. Generally, the G-band is assigned to the sp^2 trigonal bonding (graphite phase), while the D-band is attributed to the "disordered carbon", i.e. the bond angle disorder in the sp^2 microdomains, induced by linking with sp^3 carbon atoms [31,32]. The significant shift of the deconvoluted G-peak center (1510 cm^{-1}) from graphite (1580 cm^{-1}) indicates that the film has a considerable amount of sp^3 carbon bonds [7]. It should be noted also that the obtained spectrum is similar to that of the DLC films produced by PLD, where predominantly sp^3 hybridization of carbon bonding was established [33].

In the Raman spectra of the films deposited at 300 and 500 °C, instead, both G- and D-bands are clearly visible. The G- and D-peaks were deconvoluted (see Fig. 1(B)–(D)) using a Gaussian line shape, in order to obtain the I_D/I_G ratio (reported in Table 1 for all the film samples), which is proportional to the sp^2/sp^3 ratio and, as well as the G-peak position, being the most important parameter to evaluate the DLC film structure [34–36]. According to the well accepted Beeman's

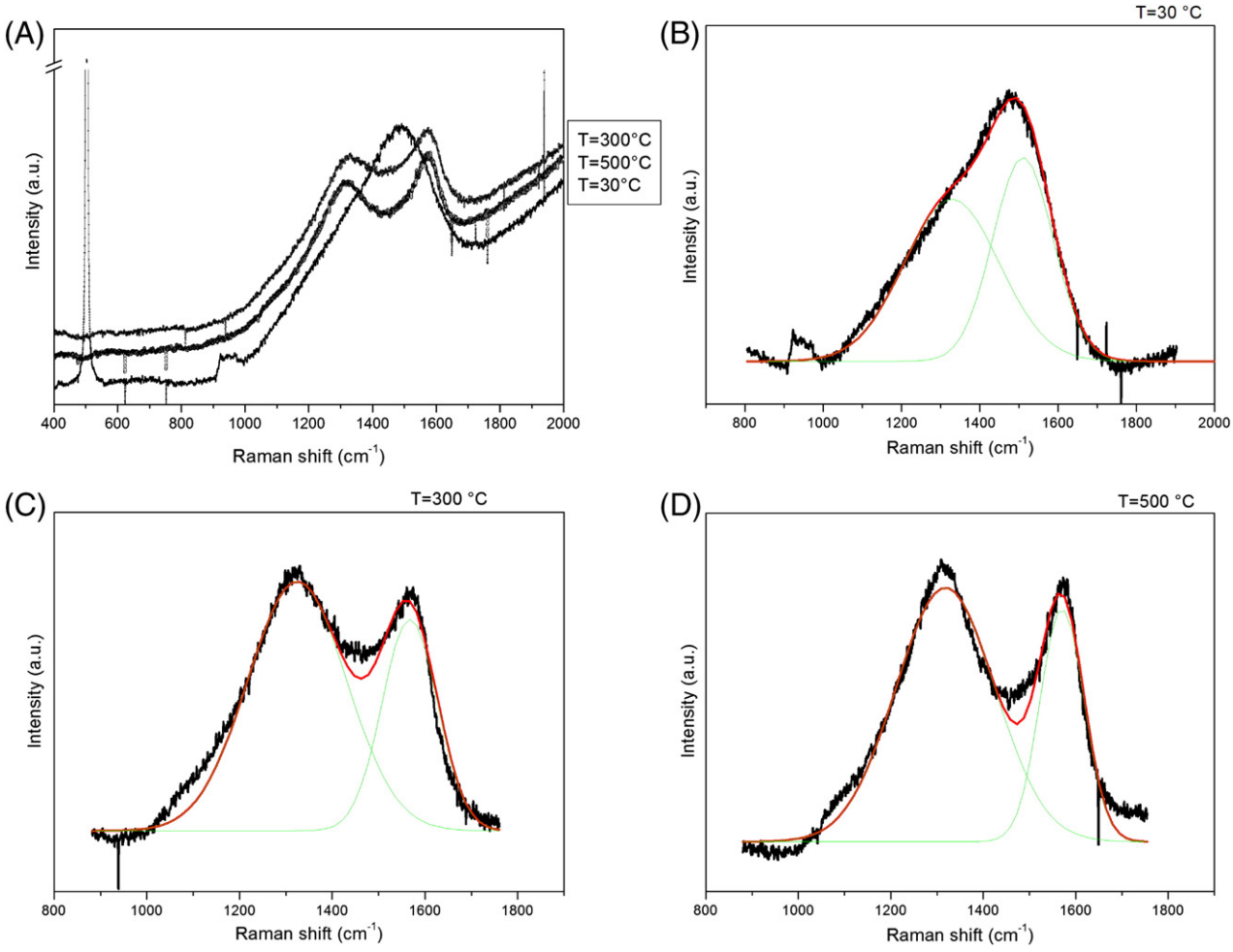

Fig. 1. (A) Raman spectra of films deposited at 30, 300 and 500 °C; deconvoluted D- and G-peaks (B) 30 °C, (C) 300 °C and (D) 500 °C.

Table 1
G-band peak positions and I_D/I_G intensity ratio obtained from Raman spectra of deposited films.

Deposition temperature, °C	G-band peak position, cm^{-1}	I_D/I_G
30	1510	1.4
300	1568	1.9
500	1570	2.7

model, the DLC films present higher sp^3 content, as they present lower I_D/I_G ratio [34].

Comparing all the samples, one can notice that, with the increase in temperature, the D-peak position remains almost unchanged, while the shift in the G-peak position towards graphite (1580 cm^{-1}) is more considerable, indicating the decrease in the amount of the sp^3 bonding from 30 to 500 °C. For the sp^3 bonding decrease accounts also the increase in the I_D/I_G ratio. As to the presence of some amount of not decomposed C_{60} buckyballs (sp^2 type of bonding) in the deposited films, it cannot be excluded, since the literature Raman spectrum of pristine C_{60} shows its most intense mode at 1465 cm^{-1}, corresponding to the pentagonal pinch mode (the A_g internal C_{60} mode) and the bands around 1420 and 1570 cm^{-1}, corresponding to the H_g symmetry modes of C_{60} [37], all being exactly in the range of broad and intense D- and G-bands of our films.

The sp^3/sp^2 ratio is one of the most important parameter defining the quality of DLC films. In general, the higher this ratio is, the closer DLC film properties approach those of diamond. To get the quantitative results of film composition, XPS analysis was carried out. The sp^3 fraction of the DLC films was deduced from XPS fitting for C1s core peak, having contributions of diamond phase (sp^3 carbon), graphite phase (sp^2 carbon) and C-bonded to O in carbonaceous contamination. The amount of carbonaceous contamination is similar in all the samples and is around 14% of the C1s peak area. The obtained binding energies (experimental error about 0.2 eV), in good agreement with those reported elsewhere [31,32,38], are presented in Table 2, while the FWHM is fixed at 1.3 eV and 1.4 eV for sp^2 and sp^3 carbon, respectively. The O1s peak at 531 eV, also present in the XPS spectra, is due to the chemisorbed oxygen species. If we assume that all the oxygen atoms in our film samples are of the same hybridization type, the O1s position can be considered as reference to correct the charging effect.

Since the area of each peak is directly related to the concentration of the corresponding phase, the sp^3 content was estimated from the ratio of the diamond peak area over the sum of the sp^2 and sp^3 peaks area. The so-obtained sp^3 percentage ranged from 46% in the 30 °C deposited film to 38% in the film deposited at $T = 300$ °C and 31% in the film deposited at $T = 500$ °C (Fig. 2(A–C)). The uncertainty in the reported values was about 10%.

The results obtained by Raman and XPS methods are in good agreement with the XAES data. The first derivate of the XAES C KLL spectra associated with the DLC films are presented in Fig. 3(A). Performing the Lascovich analysis [39], the *D*-value, representing the energy separation in eV between the major negative-going and positive-going excursion in the first derivative XAES spectra, was measured for each sample. For carbon species this energy separation indicates whether the carbon is involved in sp^2 or sp^3 bonding. Carbon with sp^2 bonding gives a wide energy separation of approximately 20 eV, in contrast, carbon with sp^3 bonding yields a narrower energy separation of about 14 eV. The increase in *D*-value could so be associated to the increasing number of pπ electrons or sp^2 sites in the film. For our films, the *D*-value varied from 18.2 eV in the 30 °C deposited film, to 19.8 eV for the film deposited at 500 °C. In Fig. 3(B), *D*-value *vs* sp^3 percentage evaluated by XPS C1s core level spectra analysis is reported. The experimental data are in good agreement with the literature data reported elsewhere [38,39].

To deposit DLC coatings, authors [4] investigated the substrate temperature range from −198 to +400 °C. It was ascertained, however, that for DLC coatings preparation the temperature should be between +20 and +75 °C, while the films deposited at elevated temperatures

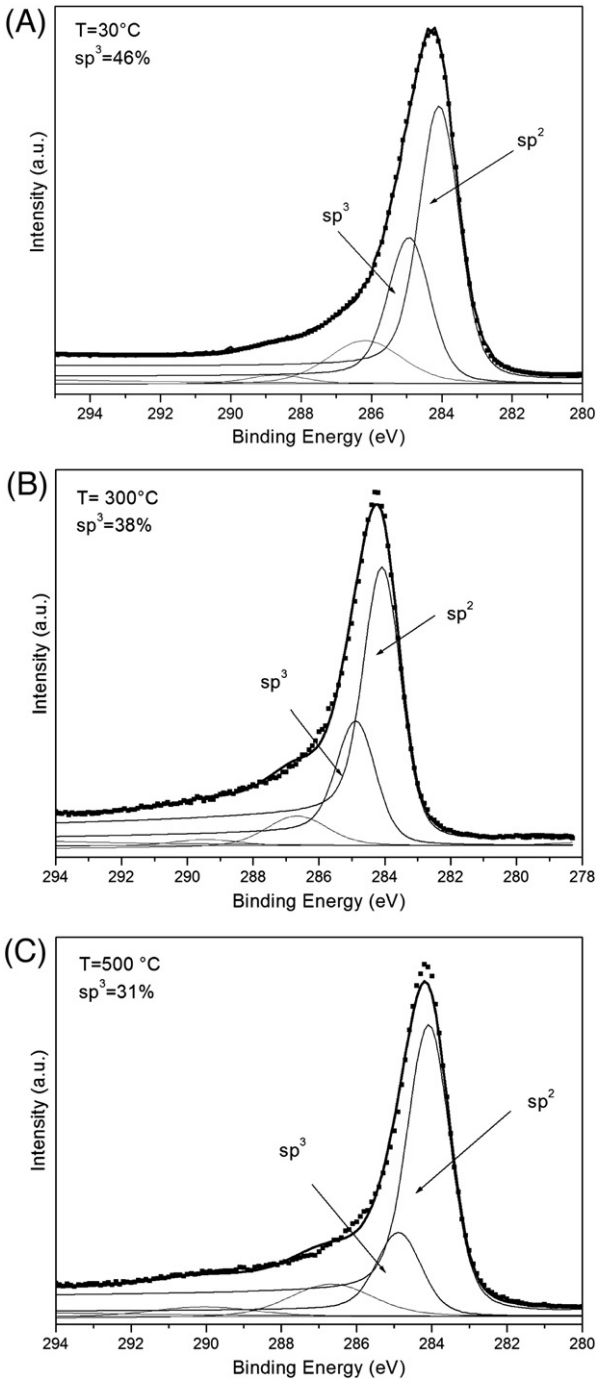

Fig. 2. XPS spectra of films deposited at: (A) 30, (B) 300 and (C) 500 °C.

Table 2
Binding energies obtained from XPS analysis of deposited films.

Binding energy, eV	$T = 30$ °C	$T = 300$ °C	$T = 500$ °C
C1s (sp^2)	284.1	284.0	284.1
C1s (sp^3)	285.2	285.0	284.9
CO	286.7	286.7	286.7
COO	290.0	289.4	290.1

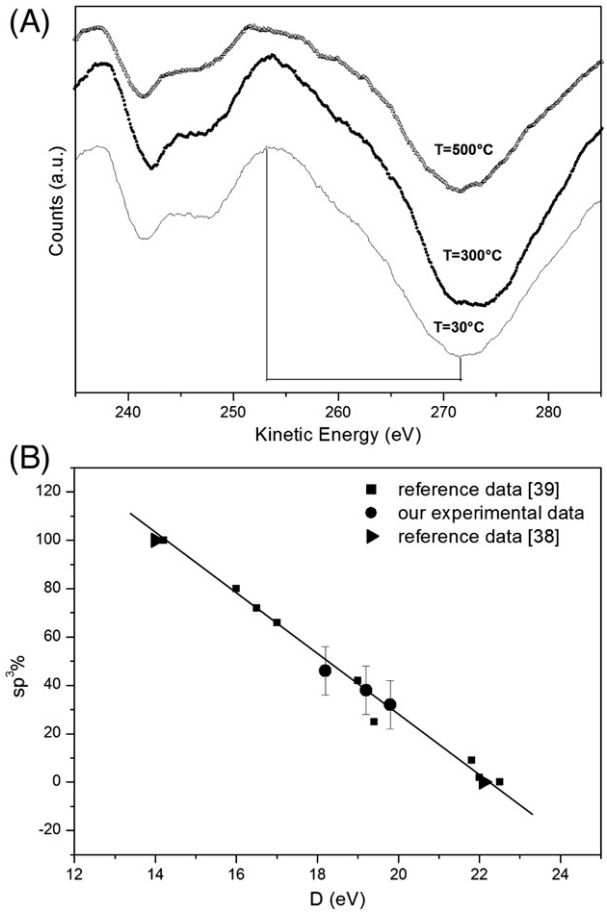

Fig. 3. (A) XAES spectra of films deposited at 30, 300 and 500 °C; (B) XPS evaluated *D*-values *vs* the sp^3 amount.

(300 °C) are graphitic in structure. A degradation of diamond-like character with the increase in the substrate temperature above 20 °C, and a transition of film properties from DLC to graphitic in the range of 150–200 °C was indicated. In our case, according to the results of Raman, XPS and XAES analysis, DLC films can be produced up to 500 °C of substrate temperature, and only the decrease in sp^3/sp^2 ratio with the increase of temperature is observed.

The Energy Dispersive X-Ray Diffraction method was applied in this work to provide information on the structure of the deposited films. Preliminary, EDXRD measurements were performed on the pristine C_{60} powder. The results, reported in Fig. 4, demonstrate that the powder is characterized by a face-centered-cubic (fcc) crystalline structure, in accordance with the literature [40] (Sys. cubic, S.G. F, card number 44-0558). Subsequently, the films deposited at 30, 300 and 500 °C were investigated. For each film sample, a series of EDXRD patterns were collected, at several scattering angles, in order to explore a wide q-range and to detect the possible Bragg contributions. Indium K_α and K_β fluorescence lines were detected at an energy of 22.1 KeV and 24.9 KeV, respectively (see the insert of Fig. 5), arising from the p-doped Si (111) substrate.

Once the optimal experimental conditions were set ($E=55$ KeV, scattering angle $2\vartheta=6.00°$, collimation slits aperture 300 μm*300 μm), the EDXRD patterns were collected in the reflection geometry and in symmetric conditions (asymmetry parameter $\alpha=0.00°$), maximizing the Si(111) contribution detected at $q=2.008\,A^{-1}$ and labelled in Fig. 5. For the 30 °C and the 300 °C deposited films, no crystalline contributions were detected. Conversely, the film grown at 500 °C shows several C_{60} reflections, labelled in the insert of Fig. 5. They correspond to the cubic face centered phase [40] (card number 44-0558). In order to maximize

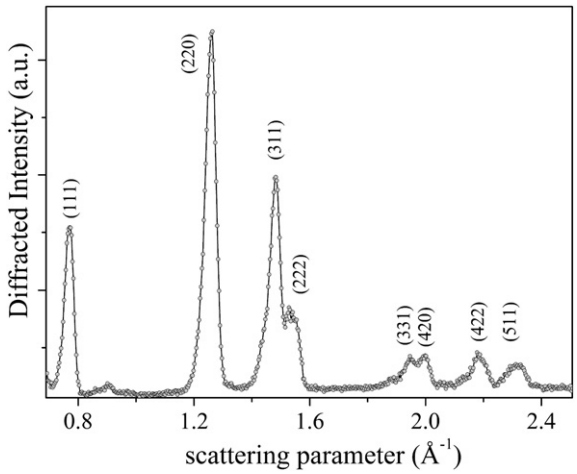

Fig. 4. EDXRD powder diffraction pattern of pristine C_{60}.

the film contribution with respect to the substrate, the Rocking Curve analysis, in the $(-2°<\alpha<2°)$ range, was performed for all the film samples. The sequence of patterns, collected under the same experimental conditions at increasing values of the asymmetry parameter, are characterized by vanishing of the Si(111) contribution. Nevertheless, no Bragg reflection from the film was detected for both the 30 and 300 °C samples, confirming that the films are not crystalline. In particular, in the case of the 500 °C deposited film, the RC analysis was performed to evaluate the film texture and the degree of epitaxy. However, the rocking curve was found to be flat, and therefore, no presence of a preferential growth direction was detected in the crystalline domain distribution. Moreover, using the Laue formulae (the Energy Dispersive analogous of the Sherrer formula, usually adopted for the conventional Angular Dispersive X-Ray diffraction [41]), it was possible to deduce the crystallites size: the nanometric dimension is in the 30/50 nm range, depending on the reflection taken into account for the fit (namely, the (220) reflection or the (331) reflection, respectively).

To correlate composition and structural properties of the prepared films with their morphological characteristics, SEM and AFM analyses were performed (Figs. 6–8). As one can see from the SEM images presented in Figs. 6(A) and 7(A), the morphology of films deposited at 30 and 300 °C, respectively, is similar and presents an amorphous

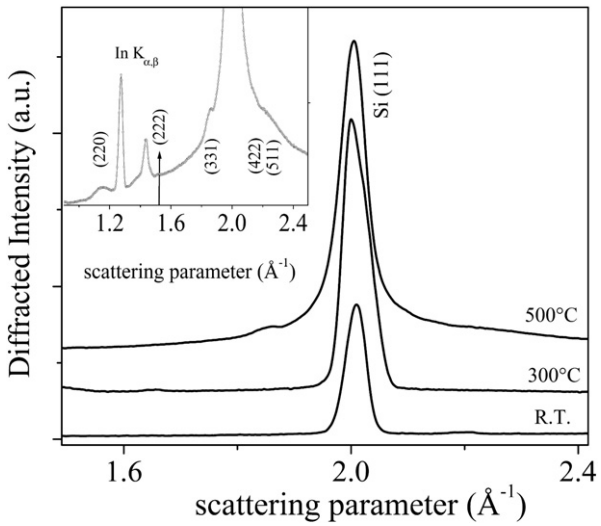

Fig. 5. EDXRD patterns collected from the carbon films deposited at 30, 300 and 500 °C. In the inset, the pattern of the 500 °C deposited film, collected at 2° of asymmetry parameter, is shown.

carbon matrix with the embedded diamond-like carbon structures, in accordance with the results of Raman, XPS and XAES analyses, with the difference that, at 300 °C, less diamond-like inclusions are visible. It can be noticed that the surface of the film deposited at 30 °C is characterized by the formation of aggregate-like structures, visible in the SEM image (Fig. 6(A)) and better evidenced by zooming of the AFM image (Fig. 6(B)). The characteristic aggregate dimensions are in the range of 30–40 nm (vertical dimension) and of 100–200 nm (lateral dimension). The average surface roughness (rms) ranges from 9 to 14 nm. As can be distinguished in Fig. 6(B), the aggregates exhibit a substructure, i.e. are composed of spherical particles, as evidenced by the line profile, of about 10 nm vertical dimension and of 50 nm lateral dimension. The film deposited at 300 °C is less homogeneous, and no aggregates of characteristic shape and dimensions can be detected, as better evidenced in Fig. 7(B). Moreover, the overall surface topography is more disordered, giving rise to an average roughness as high as ca. 25 nm.

At 500 °C (Fig. 8) of deposition temperature, a drastic surface morphology change is observed, the film is dense and compact presenting a globular morphology with some nanotube-structures visible on the surface (Fig. 8(A)). This film, with a highly textured surface composed of globular aggregates, has the morphological characteristics of a fullerene film [18,42]. The globular shaped aggregates have dimensions ranging from 30 nm (corresponding to about 300 C_{60} units) up to much larger spheres of about 500 nm (corresponding to about 5000 C_{60} units). This result is in accordance with the EDXRD one, considering that the limited

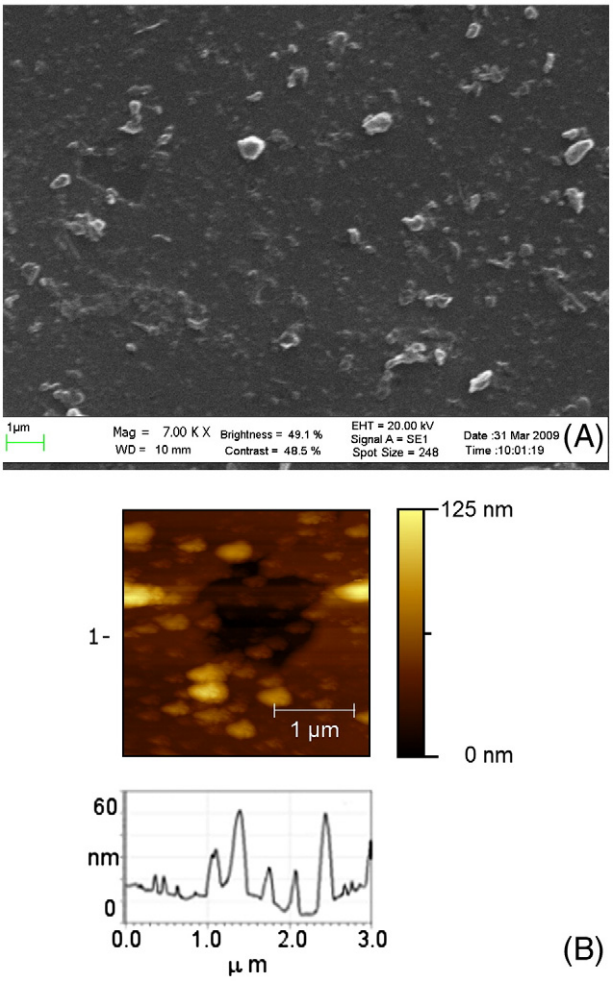

Fig. 6. SEM (A) and AFM (B) images of carbon films deposited at 30 °C. The line profile was deduced from the AFM image in correspondence to the horizontal line crossing point 1.

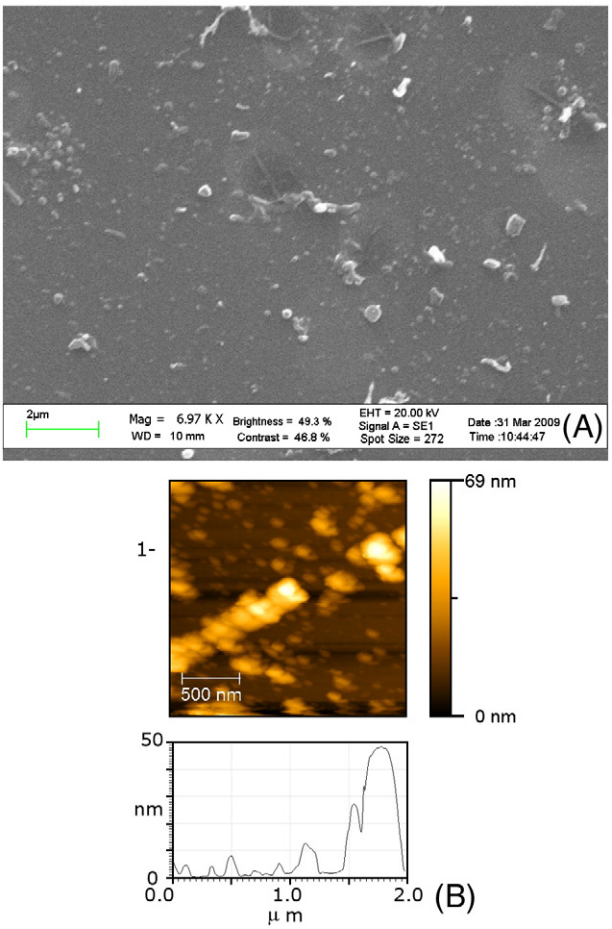

Fig. 7. SEM (A) and AFM (B) images of carbon films deposited at 300 °C. The line profile was deduced from the AFM image in correspondence to the horizontal line crossing point 1.

resolution of the latter technique did not allow the estimation of grains larger than 200 nm. The average rms ranges between 20 and 50 nm, depending on the globular aggregate dimensions. Nevertheless, in this case the roughness depends on the elevated texture of the film, while in the film deposited at 300 °C, similar rms values were defined only by a disordered growth.

Consistent results of the film thickness measurements obtained by SEM and AFM techniques are summarised in Table 3. As one can see, at 30 °C, the film is about 0.6 μm thick, while, at higher temperatures, the thickness is slightly decreased (0.5 μm), being however almost the same within the uncertainty limits (±0.1 μm).

Finally, to examine the mechanical properties of the films, Vickers microhardness measurements were carried out. In Fig. 9, the experimental plots of composite Vickers hardness (H_c) *vs* the inverse imprint diagonal (*1/D*) for the 30 and 300 °C deposited film samples are shown. The plot, corresponding to the 500 °C deposited film is not presented here, since it is very similar to that deposited at 300 °C. Calculated intrinsic hardness values for the films on Si substrates deposited at different temperatures are summarized in Table 3. As can be seen, the intrinsic hardness of film deposited at 30 °C is very high −80 GPa. The film deposited at 300 °C is still hard (35 GPa), although its hardness is more than 2 times lower than that of the film deposited at 30 °C, while the hardness of film deposited at 500 °C (29 GPa) is close to that deposited at 300 °C. The coatings are classified as superhard if possessing the hardness exceeding 40 GPa (while diamond is 100 GPa). Therefore, our DLC film deposited at 30 °C may be classified as superhard, while the other two depositions (300 and 500 °C) are hard (35 and 29 GPa, respectively).

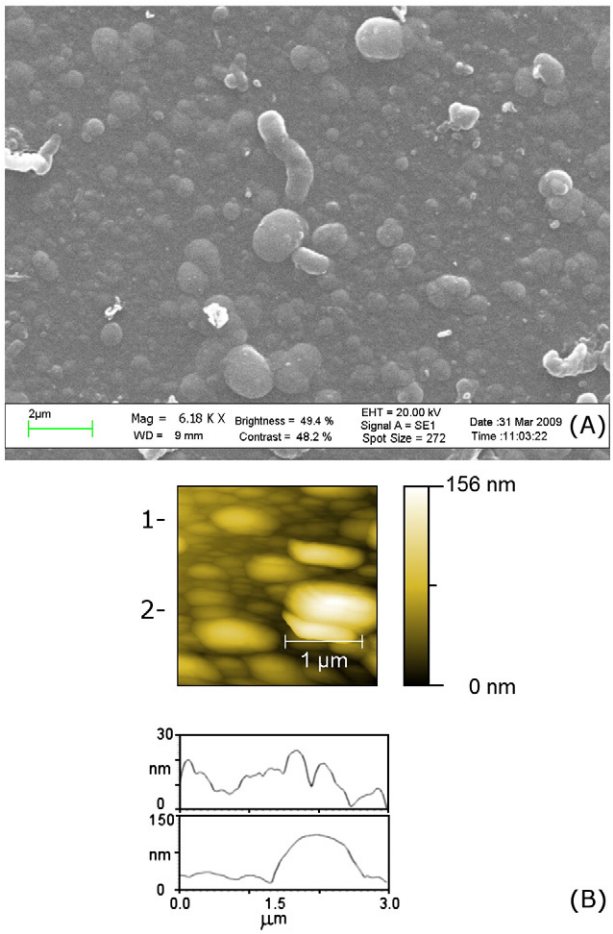

Fig. 8. SEM (A) and AFM (B) images of carbon films deposited at 500 °C. The line profiles were deduced from the AFM image in correspondence to the horizontal lines crossing points 1 and 2.

Likely, the enhanced hardness of the film deposited at 30 °C could be justified by its diamond-like nature, and the presence of 46% of sp^3 carbon bonding. There are numerous literature data reporting hard and superhard DLC coatings [4,6,8,33,43]. For example, pulsed laser irradiation of carbon targets in vacuum allowed to produce DLC with high sp^3 fraction 75–95% and a hardness of 70–100 GPa [4]. Comparing these data with our deposition at 30 °C, DLC films with lower sp^3 fraction (46%) and approximately the same hardness (80 GPa) were obtained in this work.

The authors [33] prepared 0.7 μm DLC films, characterized by 52 GPa hardness, while in [8], 55–65 GPa hardness of pulsed laser deposited DLC films was obtained. The authors [6,43] reported for 0.5 μm thick DLC coatings grown on steel substrates the hardness of 55–70 GPa.

Instead, there are very few literature data reporting the hardness of C_{60} films. The C_{60} films deposited in [44] exhibit a very low hardness (0.6 GPa), while, in [45], the reported hardness is even lower (0.2 GPa). Our data are much different: 500 °C deposited film possesses high hardness (29 GPa), likely, because our film is composed not only of C_{60}, but contains also the DLC contribution (with 31% of sp^3 fraction).

Table 3
Hardness of films on Si(111) substrates deposited at different temperatures.

Substrate temperature, °C	Thickness, μm	Vickers hardness, GPa
30	0.6 ± 0.1	80 ± 15
300	0.5 ± 0.1	35 ± 6
500	0.5 ± 0.1	29 ± 6

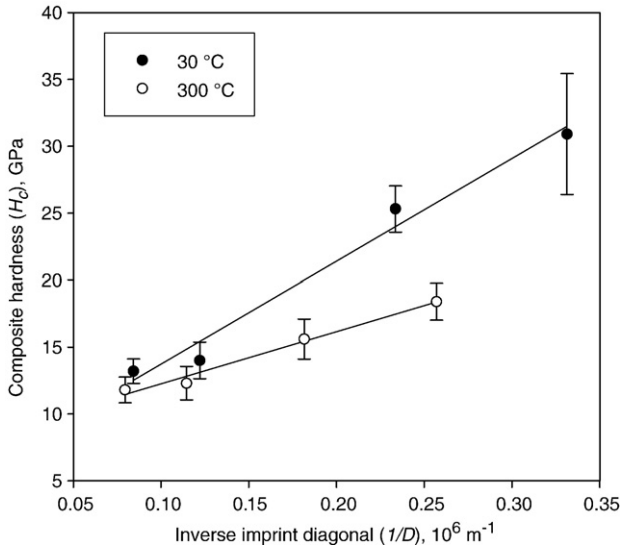

Fig. 9. Experimental plots of Vickers hardness (H_v) *vs* the inverse imprint diagonal ($1/D$) for the 30 and 300 °C deposited films.

4. Conclusions

PLD was applied to deposit carbon films from C_{60} target at different substrate temperatures. The composition, structure and morphology of films were remarkably dependent on the temperature. The results obtained by numerous techniques are all in good agreement and support each other. Upon increasing the substrate temperature from 30 to 500 °C, films of different nature were grown. At 30 and 300 °C, the obtained films are entirely amorphous DLC, with a medium degree of tetrahedral coordination, the sp^3 fraction ranging from 46% to 38%, respectively. At 500 °C, films with the coexistence of amorphous DLC (31% of the sp^3 fraction) and crystalline C_{60} are grown. This latter result evidences the fact that at 500 °C the film partially retains the C_{60} structure of the target, i.e. only partial disintegration of the C_{60} molecule upon the PLD process takes place.

SEM and AFM data suggest that the film deposited at 300 °C is topographically nonhomogeneous with average roughness of 25 nm, while in the 30 °C deposited film the aggregates of characteristic shape in the range of 30–40 nm (vertical dimension) and of 100–200 nm (lateral dimension) and average surface roughness of 9–14 nm are present. At 500 °C characteristic globular shaped aggregates, confirming the presence of C_{60}-clusters, are detected. The aggregates dimensions vary from 30 nm up to 500 nm, the average film surface roughness ranging between 20 and 50 nm.

Films grown on Si(111) substrates held at 30 °C exhibit super-hardness (80 GPa), while those grown at higher temperatures (300 and 500 °C) are hard (35 and 29 GPa, respectively).

Acknowledgement

N.S. Chilingarov is grateful to the Russian Foundation for Basic Research (RFBR), grant no. 08-03-01015-a, for financial support.

References

[1] F. Davanloo, E.M. Juengerman, D.R. Jander, T.J. Lee, C.B. Collins, J. Mater. Res. 5 (1990) 2398.
[2] C.Z. Wang, K.M. Ho, Phys. Rev. Lett. 71 (1993) 1184.
[3] P.C. Kelires, C.H. Lee, W.R. Lambrecht, J. Non-Cryst. Solids 164 (1993) 1131.
[4] A.A. Voevodin, M.S. Donley, Surf. Coat. Technol. 82 (1996) 199.
[5] D.L. Pappas, K.L. Saenger, J. Bruley, W. Krakow, J.J. Cuomo, T. Gu, R.W. Collins, J. Appl. Phys. 71 (1992) 5675.
[6] A.A. Voevodin, M.S. Donley, J.S. Zabinski, Surf. Coat. Technol. 92 (1997) 42.
[7] A.H. Jayatissa, F. Sato, N. Saito, J. Phys. D: Appl. Phys. 32 (1999) 1443.

[8] A.A. Voevodin, S.J.P. Laube, S.D. Walck, J.S. Solomon, M.S. Donley, J.S. Zabinski, J. Appl. Phys. 78 (1995) 4123.
[9] C. Du, X.W. Su, F.Z. Cui, X.D. Zhu, Biomaterials 19 (1998) 651.
[10] J. Cifre, M.C. Polo, G. Sanchez, A. Lousa, J. Esteve, Diamond Relat. Mater. 4 (1995) 798.
[11] W. Kraetschmer, L.D. Lamb, K. Fostiropoulos, D.R. Huffman, Nature 347 (1990) 354.
[12] J.H. Rhee, B. Ha, S.C. Sharma, Thin Solid Films 517 (2) (2008) 522.
[13] T.B. Singh, H. Yang, B. Plochberger, L. Yang, H. Sitter, H. Neugebauer, N.S. Sariciftci, Phys. Status Solidi B: Basic Solid State Phys. 244 (11) (2007) 3845.
[14] H. Tanimoto, K. Yamada, H. Mizubayashi, Y. Matsumoto, H. Naramaoto, S. Sakai, Appl. Phys. Lett. 93 (15) (2008) 151919/1.
[15] T.B. Singh, N.S. Sariciftci, H. Yang, L. Yang, B. Plochberger, H. Sitter, Appl. Phys. Lett. 90 (21) (2007) 213512/1.
[16] N. Kojima, Y. Suguira, M. Yamaguchi, Sol. Energy Mater. Sol. Cells 90 (2006) 3394.
[17] A. Khan, N. Kojima, M. Yamaguchi, K.L. Narayanan, O. Goetzberger, J. Appl. Phys. 87 (9, Pt. 1) (2000) 4620.
[18] L. Grausova, J. Vacik, V. Vorlicek, V. Svorcik, P. Slepicka, Diamond Relat. Mater. 18 (2–3) (2009) 578.
[19] J.E. Castle, A.M. Salvi, J. Electron Spectrosc. Relat. Phenom. 114–116 (2001) 1103.
[20] R. Felici, F. Cilloco, R. Caminiti, C. Sadun, V. Rossi, Technique for diffraction e reflection measurements of solid and liquid samples, Italian Patent No. RM 93 A 000410, 1993.
[21] R. Caminiti, V. Rossi Albertini, Int. Rev. Phys. Chem. 18 (1999) 263.
[22] B. Paci, A. Generosi, V. Rossi Albertini, E. Agostinelli, G. Varvaro, D. Fiorani, Chem. Mater. 16 (2004) 292.
[23] A. Cricenti, R. Generosi, Rev. Sci. Instrum. 66 (1995) 2843.
[24] D. Ferro, R. Scandurra, A. Latini, J.V. Rau, S.M. Barinov, J. Mater. Sci. 39 (2004) 329.
[25] D. Ferro, J.V. Rau, V. Rossi Albertini, A. Generosi, R. Teghil, Surf. Coat. Technol. 202 (2008) 1455.
[26] B. Joensson, S. Hogmark, Thin Solid Films 114 (1984) 257.
[27] A. Iost, R. Bigot, Surf. Coat. Technol. 80 (1996) 117.
[28] F. Froehlich, P. Grau, W. Grellman, Phys. Status Solidi, A 42 (1977) 79.
[29] A.M. Korsunsky, M.R. McGurk, S.J. Bull, T.F. Page, Surf. Coat. Technol. 99 (1998) 171.
[30] E.S. Puchi-Cabrera, Surf. Coat. Technol. 160 (2002) 177.
[31] N. Paik, Surf. Coat. Technol. 200 (2005) 2170.
[32] J. Filik, P.W. May, S.R.J. Pearce, R.K. Wild, K.R. Hallam, Diamond Relat. Mater. 12 (2003) 974.
[33] A.A. Voevodin, J.G. Jones, T.C. Back, J.S. Zabinski, V.E. Strel'nitzki, I.I. Aksenov, Surf. Coat. Technol. 197 (2005) 116.
[34] T.M. Manhabosco, I.L. Muller, Appl. Surf. Sci. 255 (2009) 4082.
[35] J.X. Liao, E.Q. Li, Z. Tian, X.F. Pan, J. Xu, L. Jin, H.G. Yang, J. Phys. D 41 (2008) 055305/1.
[36] S. Prawer, K.W. Nugent, Y. Lifshitz, G.D. Lempert, E. Grossman, J. Kulik, I. Avigal, R. Kalish, Diamond Relat. Mater. 5 (1996) 433.
[37] N. Bajwa, K. Dharamvir, V.K. Jindal, A. Ingale, D.K. Avasthi, R. Kumar, A. Tripathi, J. Appl. Phys. 94 (1) (2003) 326.
[38] P. Merel, M. Tabbal, M. Chaker, S. Moisa, J. Margot, Appl. Surf. Sci. 136 (1998) 105.
[39] J.C. Lascovich, R. Giorgi, S. Scaglione, Appl. Surf. Sci. 47 (1991) 17.
[40] International Centre for Diffraction Data, Database JCPDS 2000.
[41] J.V. Rau, D. Ferro, M.B. Falcone, A. Generosi, V. Rossi Albertini, A. Latini, R. Teghil, S.M. Barinov, Mater. Chem. Phys. 112 (2008) 504.
[42] E. Alvarez-Zauco, H. Sobral, E.V. Basiuk, J.M. Saniger-Blesa, M. Villagran-Muniz, Appl. Surf. Sci. 248 (2005) 243.
[43] A.A. Voevodin, M.S. Donley, J.S. Zabinski, J.E. Bultman, Surf. Coat. Technol. 76-77 (1-3, Pt. 2) (1995) 534.
[44] V.E. Pukha, A.N. Drozdov, A.T. Pugachev, S.N. Dub, Funct. Mater. 14 (2) (2007) 209.
[45] A. Richter, R. Ries, R. Smith, M. Henkel, B. Wolf, Diamond Relat. Mater. 9 (2000) 170.